

Proceedings of the Research Institute of Atmospheric,
Nagoya University, vol. 19 (1972)

ON THE REFLECTION OF WHISTLER MODE WAVES FROM MODEL LOWER IONOSPHERES

Masashi HAYAKAWA and Jinsuke OHTSU

Abstract

This paper deals with the analytical study of the effect of fine structure of the lower ionosphere on the reflection of very low frequency radio waves. We consider the case of a plane whistler wave propagating in the vertical direction in the presence of a uniform magnetic field of the same direction. The lower ionospheric model adopted here is a bilinear (double linear) density profile as a kind of idealizations of the actual ionosphere. For the bilinear model, the frequency characteristics of reflection coefficient will be shown for several combinations of β_1 and β_2 , which are the density gradients of the lower and upper layers. In these cases, conspicuous changes in reflection coefficient arise, being composed of the reduction in reflection coefficient at all frequencies and components which oscillate with frequency. Such oscillatory fluctuations with frequency may result from the wave interference effect between the penetrating and reflected waves in the lower layer.

1. Introduction

Penetration characteristics of very low frequency radio waves through the lower ionosphere have been receiving considerable attention of radio scientists and geophysicists. This work gives the detailed information on how much rate of radio wave energy generated below the ionosphere by such as lightning discharges transmits into the magnetosphere in whistler mode, and become the magnetospheric energy source. So far a number of authors have analysed this problem. *Budden* (1951), *Wait and Perry* (1957), *Johler and Walters* (1960), and *Maeda and Oya* (1963) treated the model of the simplest sharply bounded homogeneous ionosphere. The horizontally stratified isotropic models have been considered in the works of *Wait and Walters* (1963), and *Wait* (1965). Recently *Pitteway and Jespersen* (1966) have made the full-wave numerical calculations on reflection from and transmission through some model ionospheres of v. l. f. waves. *Thomas* (1969) investigated the influence of ions on reflection coef-

ficient by making use of *Pitteway's* method. And these researchers emphasized the importance of the structure of inhomogeneity.

So it is worth examining the effects of detailed structures of electron density variation of the lower ionosphere on reflection coefficient. In this paper we will derive the analytical reflection coefficient of right-hand circularly polarized waves propagating vertically upwards in a homogeneous magnetic field of vertical direction in model ionospheres. The advantage of analytical solutions lies in the physical insight they provide and in the ease with which the influences of a variation in the parameters can be determined. For the investigation of the sensitivity of reflection coefficient to finer details of density profile of the lower ionosphere, we consider the bilinear profile, thought to be an idealization, in comparison with the linear density profile. In the bilinear model, the composite expression of the reflection coefficient is obtained as a function of frequency, the density gradients of the lower and upper two layers, and the thickness of lower layer. The linear density model can be found as a special case of the bilinear model. When the reflection coefficients in the two cases are compared, the influences of minute profile of electron density are revealed. As we are especially concerned with the excitation of whistler modes, we treat only right-hand polarized waves in the following.

2. Whistler mode reflection coefficient for the bilinear density model ionosphere

Electron density — The electron density representations of the lower ionosphere have been obtained by means of rocket and ground observations. *Barrington and Thrane* (1962) deduced the electron density profile using the cross-modulation method. Recently *Maeda* (1969) derived the standard lower ionospheric electron density profile averaging the various rocket experimental data. According to *Barrington and Thrane*, there appeared the step-like structure in density, that is, the electron density was found to increase with considerable rate upto the altitude of 60 km, then form a plateau-like structure, and show a rapid increase thereafter. Such step-wise electron density profiles were also recognized in the work of *Maeda*. These density variations can be idealized as bilinear density profile to a considerable accuracy. So we assume the bilinear density profile as in the following form,

$$\begin{aligned} N_e(z) &= \beta_1 z & (0 \leq z \leq d) \\ &= \beta_1 d + \beta_2 (z-d) & (z \geq d) \end{aligned} \quad \dots\dots\dots (1)$$

where we have taken the plane of $z=0$ to be the boundary between free space and the lower layer, and $z=d$, the boundary between the neighboring linear density profiles. β_1 and β_2 are the parameters representing the density gradients of lower and upper layers, supposed to be positive. The lower ionosphere is highly variable, so its variability may be illustrated by means of the combinations of β_1 and β_2 .

Reflection coefficient — After establishing the height dependence of the electron density, the fields of the right-hand polarized waves in the ionosphere for the excitation from below are calculated as in *Hayakawa* (1969) (The vertical direction is taken as z-axis, and the time factor is $\exp(i \omega t)$),

$$\frac{d^2 E}{dz^2} + k_0^2 \left[1 - \frac{e^2 N_e}{m_e \epsilon_0 \omega (\omega - \omega_{He})} \right] E = 0. \dots\dots\dots (2)$$

Here m_e and e are the mass and charge of the electron, and ω and ω_{He} indicate the wave and electron cyclotron angular frequencies. In the following computations we assume $\omega_{He}/2\pi = 1$ MHz. k_0 and ϵ_0 are the wave number and dielectric constant of free space. N_e means the electron density, and $E = E_x + i E_y$. For the time being no consideration is given to the effects of ions and collisions.

In free space below the ionosphere ($z \leq 0$), the field consists of an incident wave and a reflected wave, i. e.,

$$E(\omega, z) = E_i(\omega) \exp(-i k_0 z) + E_r(\omega) \exp(i k_0 z) \dots\dots\dots (3)$$

where $E_i(\omega)$ and $E_r(\omega)$ are the amplitudes of the incident and reflected wave, being functions of frequency.

The electric field in the lower layer ($0 \leq z \leq d$) satisfying the wave equation of Eq. (2) reduces to the Bessel function by making use of the variable transformation $w = 1 + e^2 \beta_1 z / m_e \epsilon_0 \omega (\omega_{He} - \omega)$, and is given as follows (*Moriguchi et al.*, 1960).

$$E = A \sqrt{w} H_{\frac{1}{3}}^{(1)} \left(\frac{2}{3} l_1 w^{\frac{3}{2}} \right) + B \sqrt{w} H_{\frac{1}{3}}^{(2)} \left(\frac{2}{3} l_1 w^{\frac{3}{2}} \right) \dots\dots\dots (4)$$

with $l_1 = k_0 m_e \epsilon_0 \omega (\omega_{He} - \omega) / e^2 \beta_1$. A and B are the unknown constants to be determined. In the upper layer ($z \geq d$), the electric field has the form,

$$E = E_t \sqrt{u} H_{\frac{1}{3}}^{(2)} \left(\frac{2}{3} l_2 u^{\frac{3}{2}} \right) \dots\dots\dots (5)$$

where $l_2 = k_0 m_e \epsilon_0 \omega (\omega_{He} - \omega) / e^2 \beta_2$ and $u = 1 + e^2 \{ (\beta_1 - \beta_2) d + \beta_2 z \} / m_e \epsilon_0 \omega (\omega_{He} - \omega)$. E_t means the amplitude of the transmitted wave. In deriving Eq. (5), the Hankel function of the second kind is only picked up, because this solution shows the wave travelling upwards at great heights, being of physical significance.

Then the application of the appropriate boundary conditions, i. e., the continuity of electric fields and of their derivatives with respect to z , at $z=0$ and $z=d$ yields the reflection coefficient as a function of frequency, β_1 , β_2 and d as follows.

$$r = \frac{\Delta_r}{\Delta} \dots\dots\dots (6)$$

where the determinant Δ is expressed by Eq. (7),

$$\begin{aligned}
& 1 \quad -H_{\frac{1}{3}}^{(1)}\left(\frac{2}{3}l_1\right) \quad -H_{\frac{1}{3}}^{(2)}\left(\frac{2}{3}l_1\right) \quad 0 \\
& ik_0 - \left[\frac{d}{dz} \left\{ \sqrt{w} H_{\frac{1}{3}}^{(1)}\left(\frac{2}{3}l_1 w^{\frac{3}{2}}\right) \right\} \right]_{z=0} - \left[\frac{d}{dz} \left\{ \sqrt{w} H_{\frac{1}{3}}^{(2)}\left(\frac{2}{3}l_1 w^{\frac{3}{2}}\right) \right\} \right]_{z=0} \quad 0 \\
\Delta = & \\
& 0 \quad \left[\sqrt{w} H_{\frac{1}{3}}^{(1)}\left(\frac{2}{3}l_1 w^{\frac{3}{2}}\right) \right]_{z=d} \quad \left[\sqrt{w} H_{\frac{1}{3}}^{(2)}\left(\frac{2}{3}l_1 w^{\frac{3}{2}}\right) \right]_{z=d} \quad - \left[\sqrt{u} H_{\frac{1}{3}}^{(2)}\left(\frac{2}{3}l_2 u^{\frac{3}{2}}\right) \right]_{z=d} \\
& 0 \quad \left[\frac{d}{dz} \left\{ \sqrt{w} H_{\frac{1}{3}}^{(1)}\left(\frac{2}{3}l_1 w^{\frac{3}{2}}\right) \right\} \right]_{z=d} \quad \left[\frac{d}{dz} \left\{ \sqrt{w} H_{\frac{1}{3}}^{(2)}\left(\frac{2}{3}l_1 w^{\frac{3}{2}}\right) \right\} \right]_{z=d} - \left[\frac{d}{dz} \left\{ \sqrt{u} H_{\frac{1}{3}}^{(2)}\left(\frac{2}{3}l_2 u^{\frac{3}{2}}\right) \right\} \right]_{z=d} \dots (7)
\end{aligned}$$

and also Δ_r is obtained by replacing the first column in Eq. (7) with the column matrix $(-1, i k_0, 0, 0)$. Further the unknown coefficients are also determined to give the field distribution in the ionosphere. The case of linear density profile is found to be a special case of the bilinear profile, i. e., corresponds to the occasion of $d=0$. So β_2 is only meaningful, and designated as β .

3. Numerical results and discussion

Variation of the reflection coefficient with frequency — In order to show the importance of the effect of density gradient of the lower ionosphere on the reflection coefficient at the beginning, we plotted in Fig. 1 the dependence of the reflection coefficient on the density gradient in the case of linear model at specific frequencies, i. e., 100, 500 Hz, 1, 5, 10 and 100 kHz. We notice that the reflection coefficient for the lower frequencies takes greater value than that of higher frequencies. Also it is apparent that the variations for higher three frequencies are quite different from those for lower frequencies. In order of increasing the value of β , the reflection coefficients at 100, 500 Hz and 1 kHz show the considerably sharp enhancements in the range from 10^3 to 10^5 m^{-4} , then continue to increase gradually. On the other hand, the coefficient for 5 kHz increases slowly until around the β value of 10^4 m^{-4} , thereafter indicates a relatively abrupt rise in magnitude as to attain the value of

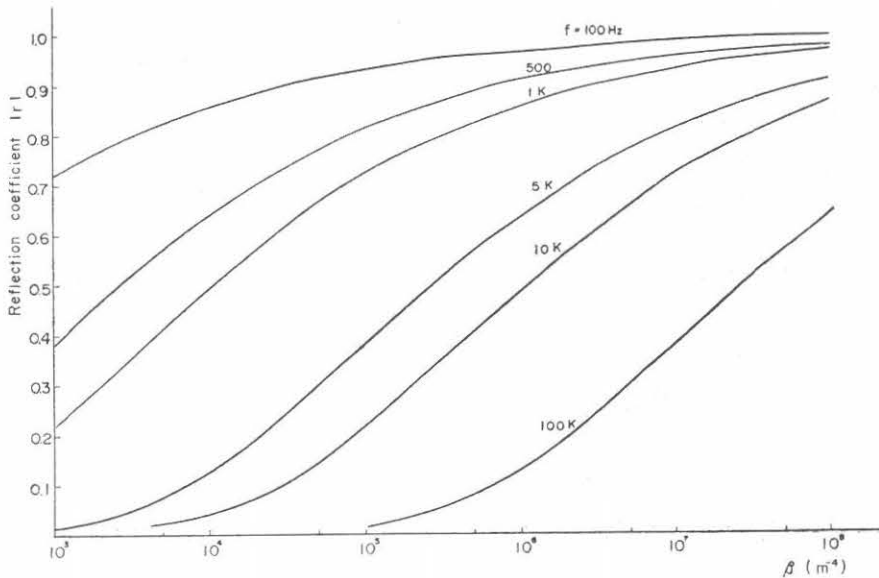


Fig. 1. Variation of the reflection coefficient with density gradient in the case of linear density model.

~ 0.9 at $\beta = 10^8 \text{ m}^{-4}$. Similar tendencies are found at the frequencies of 10 and 100 kHz, though the curves show rightward shift in β with respect to the variation for 5 kHz owing to the enhanced frequency. Fig. 1 implies that we must take into account the finer structure of the lower ionosphere. So we turn our attention to the case of bilinear density model.

In Figs. 2 through 6 we have plotted the magnitude of the reflection coefficient $|r|$ against frequency for cases of various combinations of β_1 and β_2 . Combination of β_1 and β_2 depends on the local time of the day, season, year and solar activity etc., which is not discussed in detail here. And the thickness of the lower layer, d , is left as a parameter. In order to lessen the disagreement between the model and real ionospheres, we choose the value of β_1 being smaller than that of β_2 . Figures 2 and 3 are the numerical results for $\beta_2 = 10^5$ and 10^6 m^{-4} , respectively when $\beta_1 = 10^8 \text{ m}^{-4}$. A simple comparison of these figures with the case of $d = 0 \text{ km}$, i. e., only the upper layer of linear model, shows that the most striking effect of the introduction of the lower layer in the two-layer model is the depression of the coefficient and making the coefficient fluctuate with frequency. When the thickness of the lower layer, d , is relatively small, the fluctuation with frequency is trivial. However, for d being over 20 km, such effects become remarkable. These changes are conspicuous especially in the frequency range from a few 100 Hz to several kHz. In the curves for $d = 40 \text{ km}$ in the two figures, we can see some maximums and minimums, though not so clear.

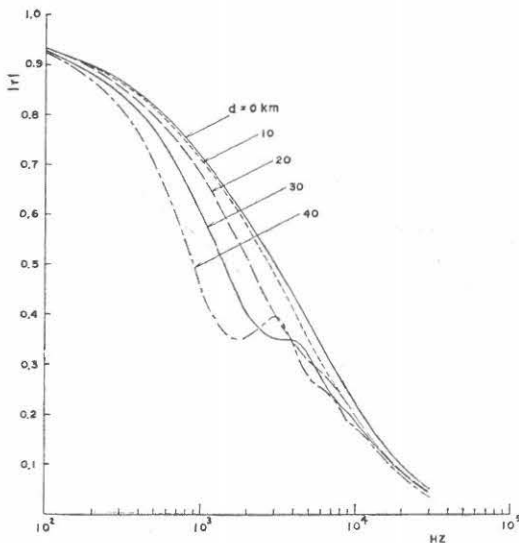


Fig. 2. Frequency characteristic of the reflection coefficient for the bilinear model when $\beta_1 = 10^8$ and $\beta_2 = 10^5 \text{ m}^{-4}$.

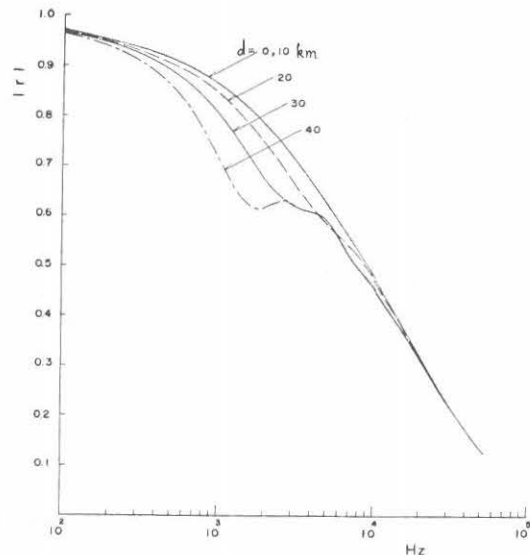


Fig. 3. Frequency characteristic of the reflection coefficient when $\beta_1 = 10^8$ and $\beta_2 = 10^6 \text{ m}^{-4}$.

Figs. 4, 5, and 6 are the frequency characteristics of the reflection coefficient with $\beta_1 = 10^4 \text{ m}^{-4}$ for three specific values of β_2 , i. e., 10^5 , 10^6 and 10^7 m^{-4} . Although the reduction in $|r|$ at all frequencies compared with the result of the upper layer only (i. e. $d = 0 \text{ km}$) occurs, being the same with the cases of Figs. 2 and 3, it appears that the frequency dependences are quite different from Figs. 2 and 3, and they are composed of considerably complicated variations due to the increased value of β_1 . Such fluctuating changes may result from the wave interference in the lower layer between the upgoing waves and reflected waves from the boundary of the two layers. It is found that the change of the reflection coefficient in Figs. 4 shows somewhat a different structure from that of Figs. 5 and 6. The reason of such discrepancy may be that since the difference between the density gradients β_1 and β_2 is small compared with the cases of Figs. 5 and 6, the amplitude of reflected waves is relatively small, so causing a slight wave interference effect. Changing the value of d is expected to show us some different interference patterns, since the thickness depends on the phase difference between the penetrating and reflected waves. In Fig. 4, the oscillatory component is superimposed on the frequency variation with general tendency of decreasing with increasing frequency. Compared with the result of Figs. 2 and 3, we find much more complex wave interference pattern. For $d = 10 \text{ km}$, the reflection coefficient shows a relatively smooth variation with frequency. It is found that the wave interference structure for the case of $d = 20 \text{ km}$ takes the variation having two minimums at 2 kHz and 9 kHz, two maximums at 4.5 and 11 KHz, and a blunt peak around 20 kHz. The result of $d = 30 \text{ km}$ is also plotted, giving rise to an ionospheric window of nearly zero reflection coefficient near the frequency 9 kHz.

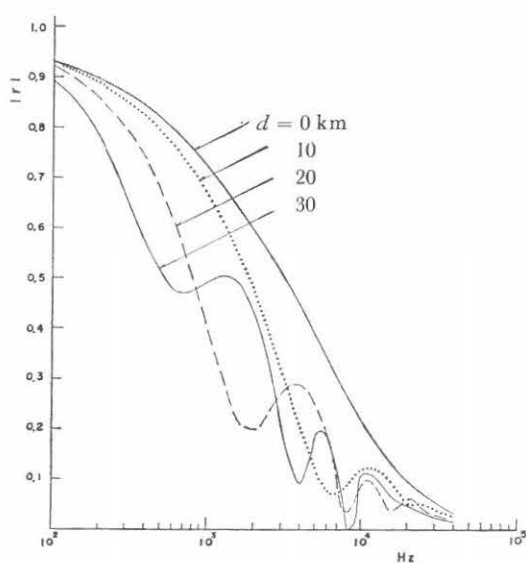


Fig. 4. Frequency characteristic of the reflection coefficient when $\beta_1 = 10^4$ and $\beta_2 = 10^5 \text{ m}^{-4}$.

The interference effect in reflection coefficient appears distinctly in Figs. 5 and 6. In Fig. 5 we have plotted $|r|$ for four specific values of d . The frequency characteristic for $d = 10$ km does not differ so much from the result of $d = 0$ km. It can be seen that the variation of the reflection coefficient with frequency takes the form of damped oscillation for the cases of $d = 20$ and 30 km. The curve of $d = 20$ km shows a pronounced minimum at 2 kHz. With special reference to the occasion of $d = 30$ km, the reflection coefficient exhibits characteristic minimums at 680 Hz, 4 and 8 kHz, considered to behave like the ionospheric windows for low frequency radio waves. The result in Fig. 6 indicates the similar variation in that the curve has some minimums, though the magnitude of the reflection coefficient takes greater value due to the enhanced β_2 . However, the characteristic minimums in higher frequency range become less pronounced. Moreover a sharp minimum can be found at the frequency of 700 Hz for $d = 30$ km. To ascertain the interference effect, we made the calculation of the height distribution of wave field intensity, which clearly showed the standing wave pattern, although not presented in this paper. It may be concluded that when β_1 is increased to the value of 10^4 m^{-4} , we can find out the interference effect, while such effect is only trivial if $\beta_1 = 10^3 \text{ m}^{-4}$. In addition, the fluctuating frequency dependence of reflection coefficient becomes more marked if the difference between the values of β_1 and β_2 is large with β around 10^4 , as inferred from Figs. 5 and 6 (Hayakawa and Ohtsu, 1972).

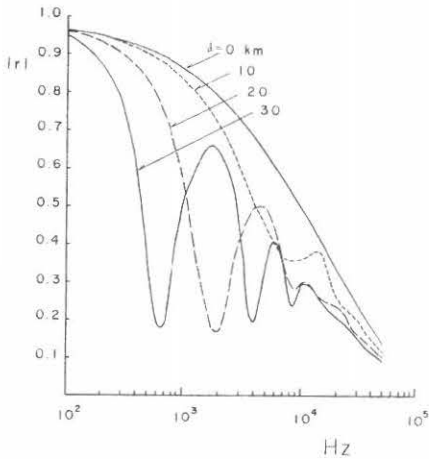


Fig. 5. Frequency characteristic of the reflection coefficient when $\beta_1 = 10^4$ and $\beta_2 = 10^6 \text{ m}^{-4}$.

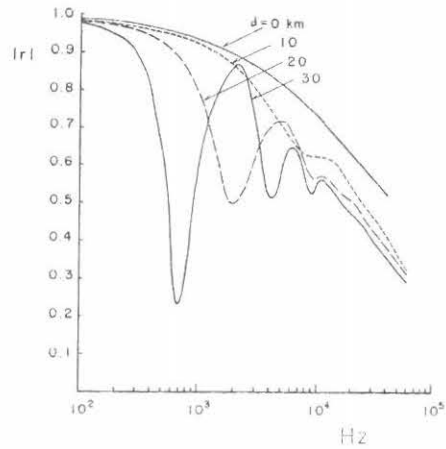


Fig. 6. Frequency characteristic of the reflection coefficient when $\beta_1 = 10^4$ and $\beta_2 = 10^7 \text{ m}^{-4}$.

The effects of ions and collisions on the reflection coefficient — So far we have neglected the influences of ions and collisions, which will be found to be of negligible order in the following. Here we assume the plasma is composed of electrons and positive ions of one kind, so the profile of electron density is considered to represent

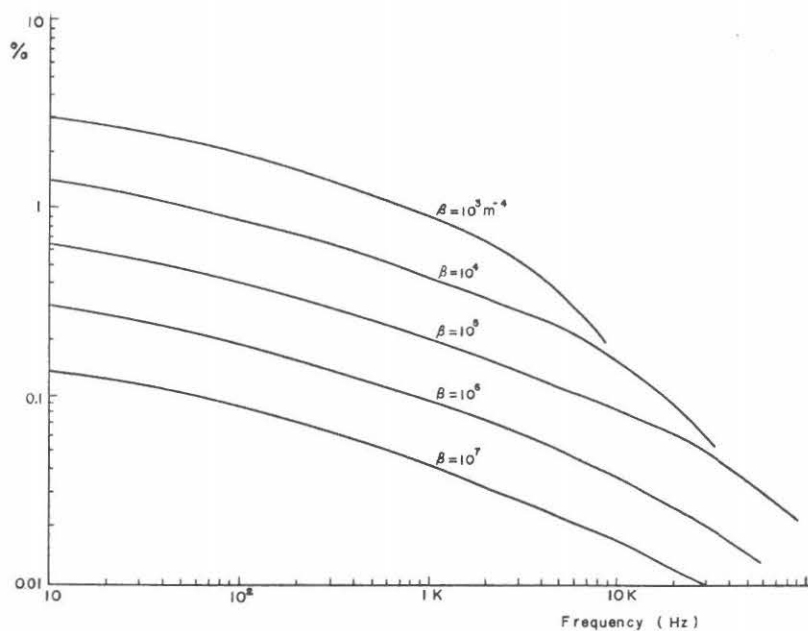


Fig. 7. Frequency dependence of the percentage decrease in reflection coefficient due to the presence of ions of a. m. u. 30.

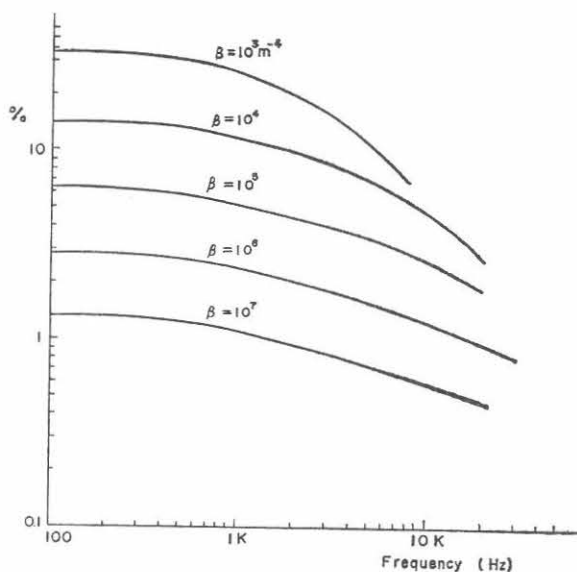


Fig. 8. Frequency dependence of the effect of proton ions.

namely that of ion density. There exist very few distinct observations and theories concerning the ion composition in the lower ionosphere (e.g., *Cole and Pierce, 1965*). Figs. 7 and 8 indicate the frequency characteristics of the ion effect on reflection coefficient. The atomic mass unit (a. m. u.) of the ion in Fig. 7 is adopted to be 30,

which seems not so unreasonable for the actual ionosphere. And the proton is taken as the positive ion in Fig. 8. Although this assumption may seem unrealistic, a comparison is made with Fig. 7. In both figures, we plotted the percentage decrease in reflection coefficient due to the presence of ions compared with the case of electron alone, against frequency only for linear density model. First glance of Fig. 7 shows that the ion effect becomes more conspicuous as β takes smaller value in the frequency range below about a few kHz. Above a few kHz the effect of inclusion of ions falls off gradually, then begins to be negligible at ~ 3 kHz for $\beta = 10^3 \text{ m}^{-4}$ and at ~ 10 kHz for $\beta = 10^4 \text{ m}^{-4}$, respectively. In order of increasing the value of β , the frequency at which the sharp reduction in ion effect occurs, seems to shift to higher value. On the other hand, when the species of the ion is changed to proton, the influence of ions is so enhanced that we must take it into consideration, as is clearly demonstrated in Fig. 8.

The inclusion of constant collision frequency is studied in the case of linear model. One example is shown in Fig. 9 when $\beta = 10^5 \text{ m}^{-4}$. It is distinctly apparent from the figure that the curves for collision frequency ν less than 10^7 sec^{-1} and those for $\nu = 10^8 \text{ sec}^{-1}$ exhibit the different variations from each other. In Fig. 9 when $\beta = 10^5 \text{ m}^{-4}$, in the frequency range less than about 10 kHz, the effect of collision is to enhance the coefficient, then over a critical frequency ~ 9 kHz the collision has the

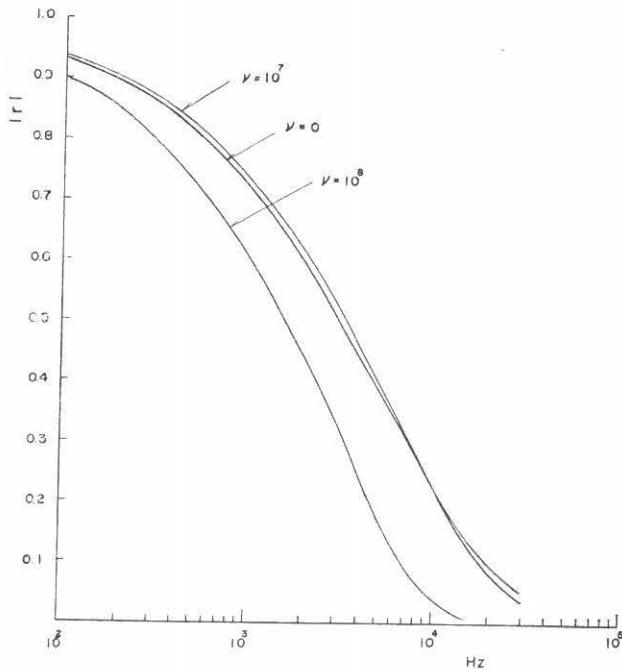


Fig. 9. Frequency characteristic of the reflection coefficient with collisional effect included for $\beta = 10^5 \text{ m}^{-4}$ in the case of linear density model.

function to depress the coefficient for ν less than 10^7 sec^{-1} . Also for $\nu = 10^8 \text{ sec}^{-1}$ the reflection coefficient is much diminished compared with that of $\nu = 0$. The critical frequency, at which the change from enhancement to reduction in coefficient occurs, is found to shift toward higher frequency as β increases, which was derived from the results for other lower β values. It is clear that this critical frequency don't appear in e. l. f. and v. l. f. range for the cases of $\beta = 10^6$ and 10^7 m^{-4} , although not shown. Generally speaking, the collisional effect can be neglected when ν is less than 10^7 sec^{-1} . Though the collisional effect was found to be of negligible magnitude in reflection coefficient, it has a serious influence on the propagation loss in the ionosphere, which was studied by the calculations of electric field intensities. So when considering the transition to whistler modes, the absorption loss may prevail over the reflection loss.

4. Conclusion

The model ionospheres used so far by many workers are of simple form, e. g., exponential, so the frequency characteristics of the reflection coefficients showed similar variations with the linear case. And such wave interference effects in reflection coefficients as indicated in the present paper have never been found. Compared with the linear model, marked changes in the case of bilinear density profile resulted in, being composed of reduction in reflection coefficient at all frequencies, and components which oscillate with frequency. Considering this fact, the fine structure of D and E layers of the lower ionosphere must be taken into account, when treating the reflection of v. l. f. and e. l. f. radio waves. Though the bilinear model we used proves to be a kind of idealizations, the real lower ionosphere shows much more complicated structure, especially during magnetically disturbed periods. So it is necessary to study the reflection problem under more accurate, though complex, ionosphere models. Further on the occasions when the reflection coefficient in e. l. f. range takes a relatively small value due to the wave interference effect, a considerable part of e. l. f. wave energy may be transmitted into the ionosphere.

References

- Barrington, R. E., and E. V. Thrane, The determination of D-region electron densities from observations of cross modulations, *J. Atmos. Terr. Phys.*, **24**, 31-43, 1962.
- Budden, K. G. The reflection of very low frequency radio waves at the surface of a sharply bounded ionosphere with superimposed magnetic field, *Phil. Mag.* 2, **42**, 833-850, 1951.
- Cole, R. K., and E. T. Pierce, Electrification in the earth's atmosphere for altitudes between 0 and 100 kilometers, *J. Geophys. Res.*, **70**, 2735-2749, 1965.

- Hayakawa, M., Propagation of whistler modes in an inhomogeneous plasma, *J. Phys. Soc. Japan*, **27**, 1373, 1969.
- Hayakawa, M., and J. Ohtsu, Wave interference effect in whistler mode reflection coefficients for model lower ionospheres, *J. Geomag. Geoelect.*, 1972 (in press).
- Johler, J. R., and L. C. Walters, On the theory of reflection of low- and very-low-radio frequencies from the ionospheres, *J. Res. N. B. S.*, **64D**, 269-285, 1960.
- Maeda, K., and H. Oya, Penetration of vlf radio waves through the ionosphere, *J. Geomag. Geoelect.*, **14**, 151-171, 1963.
- Maeda, K., Mid-latitude electron density profile as revealed by rocket experiments, *J. Geomag. Geoelect.*, **21**, 557-567, 1969.
- Moriguchi, S., K. Udagawa, and S. Hitotsumatsu, *Sagaku-Kōshiki (Mathematical formulas) 3*, Iwanami Pub. Co., 1960. (in Japanese)
- Pitteway, M. L. V., and J. L. Jespersen, A numerical study of the excitation, internal reflection and limiting polarization of whistler waves in the lower ionosphere, *J. Atmos. Terr. Phys.*, **28**, 17-43, 1966.
- Thomas, L., The effects of ions on the propagation of e. l. f. and v. l. f. waves in the ionosphere, *J. Atmos. Terr. Phys.*, **31**, 991-1002, 1969.
- Wait, J. R., and L. B. Perry, Calculation of ionospheric reflection coefficients at very low frequencies, *J. Geophys. Res.*, **62**, 43-56, 1957.
- Wait, J. R., and L. C. Walters, Reflection of vlf radio waves from an inhomogeneous ionosphere. Part I. Exponentially varying isotropic model, *J. Res. N. B. S.*, **67D**, 361-367, 1963.
- Wait, J. R., Concerning the mechanism of reflection of electromagnetic waves from an inhomogeneous lossy plasma, *J. Res. N. B. S.*, **69D**, 865-869, 1965.